Stability of an expanding circular cavity and the failure of amorphous solids

Eran Bouchbinder,[1,2] Ting-Shek Lo,[1,3] Itamar Procaccia,[1] and Elad Shtilerman[1]
[1]*Department of Chemical Physics, Weizmann Institute of Science, Rehovot 76100, Israel*
[2]*Racah Institute of Physics, Hebrew University of Jerusalem, Jerusalem 91904, Israel*
[3]*Department of Physics, The Chinese University of Hong Kong, Shatin, Hong Kong*
(Received 11 November 2007; revised manuscript received 12 June 2008; published 28 August 2008)

Recently, the existence and properties of unbounded cavity modes, resulting in extensive plastic deformation failure of two-dimensional sheets of amorphous media, were discussed in the context of the athermal shear-transformation-zones (STZ) theory. These modes pertain to perfect circular symmetry of the cavity and the stress conditions. In this paper we study the shape stability of the expanding circular cavity against perturbations, in both the unbounded and the bounded growth regimes (for the latter the unperturbed theory predicts no catastrophic failure). Since the unperturbed reference state is time dependent, the linear stability theory cannot be cast into standard time-independent eigenvalue analysis. The main results of our study are as follows: (i) sufficiently small perturbations are stable; (ii) larger perturbations within the formal linear decomposition may lead to an instability; this dependence on the magnitude of the perturbations in the linear analysis is a result of the nonstationarity of the growth; and (iii) the stability of the circular cavity is particularly sensitive to perturbations in the effective disorder temperature; in this context we highlight the role of the rate sensitivity of the limiting value of this effective temperature. Finally we point to the consequences of the form of the stress dependence of the rate of STZ transitions. The present analysis indicates the importance of nonlinear effects that were not taken into account yet. Furthermore, the analysis suggests that details of the constitutive relations appearing in the theory can be constrained by the modes of macroscopic failure in these amorphous systems.

DOI: 10.1103/PhysRevE.78.026124 PACS number(s): 62.20.M−, 64.70.Q−

I. INTRODUCTION

Some of the theoretically most fascinating aspects of crack propagation in amorphous materials are the instabilities that are observed in well controlled laboratory experiments [1]. Besides some exceptions (see, for example, [2–4] and also [5,6]), it would be fair to say that the observed instabilities are still poorly understood. It is the opinion of the present authors that the reason for the relative lack of understanding is that the theory of crack propagation did not treat cracks as moving free boundaries whose instabilities stem from the dynamics of the free boundary itself. Instead, "crack tip dynamics" were replaced by energy balance within the theory of linear elastic fracture mechanics [7], together with an ad hoc "law" of one nature or another as to where a crack is supposed to move.

In principle this undesirable state of affairs can be greatly improved within the shear-transformation-zones (STZ) theory of amorphous materials [8–11]. This theory treats developing cracks or growing cavities as free boundaries of a material in which both elasticity and plasticity are taken into account, preserving all the symmetries and conservation laws that promise a possibly correct theory of amorphous materials driven out of mechanical equilibrium. This theory in its various appearances was compared to a number of experiments and simulations (see below), with a growing confidence that although not final, STZ theory is developing in the right direction. Indeed, the application of a highly simplified version of STZ theory to crack propagation resulted in physically interesting predictions, explaining how plasticity can intervene in blunting a crack tip and resulting in velocity selection [12]. The application of the full fledged theory of STZ to crack propagation is still daunting (although not impossible) due to the tensorial nature of the theory and the need to deal with an extremely stiff set of partial differential equations with a wide range of time scales and length scales involved. For that reason it seemed advantageous to apply the full theory to a situation in which the symmetries reduce the problem to an effectively scalar theory; this is the problem of a circular cavity developing under circular symmetric stress boundary conditions [13,14]. While this problem does not reach the extreme conditions of stress concentration that characterize a running slender crack, it still raises many physical issues that appear also in cracks, in particular, the give and take between elasticity and plasticity, the way stresses are transmitted to moving boundaries (in apparent excess of the material yield stress), and most importantly for this paper, the possible existence of dynamical instabilities of the moving free boundary. This last issue might also be connected to the difference between ductile and brittle behaviors. In the former, a growing cavity is likely to remain rather smooth, whereas in the latter, one may expect an instability resulting in the growth of "fingers," possibly ending up being cracks. It is one of the challenges of the present paper to examine whether the theory may predict a transition, as a function of material parameters or a constitutive relation, between these two types of behavior.

Note that we have chosen to study the problem in a purely two-dimensional geometry; recently quasi-two-dimensional systems exhibited interesting failure dynamics in laboratory experiments, where the third dimension appears irrelevant for the observed phenomena [5,15]. Our motivation here is, however, theoretical, to reduce the unnecessary analytic and numerical complications to a minimum and to gain insight as to the main physical effects under the assumption that the

thin third dimension in real systems does not induce a catastrophic change in behavior. When this assumption fails, as it does in some examples, cf. [1], the analysis must be extended to include the third dimension. This is beyond the scope of this paper.

In Sec. II we present the equations that describe the problem at hand and specify their boundary conditions. Particular attention is paid to distinguish between the general Eulerian formulation which is model independent (Sec. II A) and the constitutive relations involving plasticity where the STZ model is explained (Sec. II B). This section finishes with the presentation of the unperturbed problem, preparing the stage for the linear stability analysis which is discussed in Sec. III. In this section we present a general analysis where inertia and elastic compressibility effects are taken into account. In Appendix B we complement the analysis by considering the "quasistatic" (when the velocity of the boundary is sufficiently small) and incompressible case (when the bulk modulus is sufficiently large) and show that both formulations agree with one another in the relevant range. The results of the stability analysis are described in detail in Sec. IV and a few concluding remarks are offered in Sec. V.

II. EQUATIONS AND BOUNDARY CONDITIONS

A. General formulation

We start by writing down the full set of equations for a general two-dimensional elastoviscoplastic material. A basic assertion of this theory is that plastic strain tensors in such materials are not state variables since their values depend on the entire history of deformation. Thus, one begins by introducing the total rate of deformation tensor

$$\mathbf{D}^{\mathrm{tot}} \equiv \frac{1}{2}[\boldsymbol{\nabla}\mathbf{v} + (\boldsymbol{\nabla}\mathbf{v})^T], \tag{2.1}$$

where $\mathbf{v}(\mathbf{r},t)$ is the material velocity at the location $\mathbf{r}$ at time t and T denotes here the transpose of a tensor. This type of Eulerian formulation has the enormous advantage that it disposes of any reference state, allowing free discussion of small or large deformations. As is required in an Eulerian frame we employ the full material time derivative for a tensor $\mathbf{T}$,

$$\frac{\mathcal{D}\mathbf{T}}{\mathcal{D}t} = \frac{\partial \mathbf{T}}{\partial t} + \mathbf{v}\cdot\boldsymbol{\nabla}\mathbf{T} + \mathbf{T}\cdot\boldsymbol{\omega} - \boldsymbol{\omega}\cdot\mathbf{T}, \tag{2.2}$$

where $\boldsymbol{\omega}$ is the spin tensor,

$$\boldsymbol{\omega} \equiv \frac{1}{2}[\boldsymbol{\nabla}\mathbf{v} - (\boldsymbol{\nabla}\mathbf{v})^T]. \tag{2.3}$$

For a scalar or vector quantity $\mathbf{V}$ the commutation with the spin tensor vanishes identically. The Eulerian approach allows a natural formulation of moving free boundary problems; this will be shown to lead to a significant advance compared to more conventional treatments.

The plastic rate of deformation tensor $\mathbf{D}^{\mathrm{pl}}$ is introduced by assuming that the total rate of deformation tensor $\mathbf{D}^{\mathrm{tot}}$ can be written as a sum of a linear elastic and plastic contributions

$$\mathbf{D}^{\mathrm{tot}} = \frac{\mathcal{D}\boldsymbol{\epsilon}^{\mathrm{el}}}{\mathcal{D}t} + \mathbf{D}^{\mathrm{pl}}. \tag{2.4}$$

We further assume that $\mathbf{D}^{\mathrm{pl}}$ is a traceless tensor, corresponding to incompressible plasticity. All possible material compressibility effects in our theory are carried by the elastic component of the deformation. The components of the linear elastic strain tensor $\boldsymbol{\epsilon}^{\mathrm{el}}$ are related to the components of stress tensor, whose general form is

$$\sigma_{ij} = -p\,\delta_{ij} + s_{ij}, \quad p = -\frac{1}{2}\sigma_{kk}, \tag{2.5}$$

according to

$$\epsilon^{\mathrm{el}}_{ij} = -\frac{p}{2K}\delta_{ij} + \frac{s_{ij}}{2\mu}, \tag{2.6}$$

where K and μ are the two-dimensional bulk and shear moduli, respectively. The tensor $\mathbf{s}$ is referred to hereafter as the "deviatoric stress tensor" and p as the pressure. The equations of motion for the velocity and density are

$$\rho\frac{\mathcal{D}\mathbf{v}}{\mathcal{D}t} = \boldsymbol{\nabla}\cdot\boldsymbol{\sigma} = -\boldsymbol{\nabla}p + \boldsymbol{\nabla}\cdot\mathbf{s}, \tag{2.7}$$

$$\frac{\mathcal{D}\rho}{\mathcal{D}t} = -\rho\,\boldsymbol{\nabla}\cdot\mathbf{v}. \tag{2.8}$$

In order to prepare the general set of equations for the analysis of a circular cavity we rewrite the equations in polar coordinates. For that aim we write

$$\boldsymbol{\nabla} = \mathbf{e}_r\partial_r + \frac{\mathbf{e}_\theta}{r}\partial_\theta, \quad \mathbf{v} = v_r\mathbf{e}_r + v_\theta\mathbf{e}_\theta, \tag{2.9}$$

where $\mathbf{e}_r$ and $\mathbf{e}_\theta$ are unit vectors in the radial and azimuthal directions, respectively. These expressions enable us to represent the divergence operator $\boldsymbol{\nabla}\cdot$ in the equations of motion and the covariant derivative $\mathbf{v}\cdot\boldsymbol{\nabla}$ in the material time derivative of vectors and tensors. Some care should be taken in evaluating these differential operators in polar coordinates since the unit vectors themselves vary under differentiation according to

$$\partial_r\mathbf{e}_r = 0, \quad \partial_r\mathbf{e}_\theta = 0, \quad \partial_\theta\mathbf{e}_r = \mathbf{e}_\theta, \quad \partial_\theta\mathbf{e}_\theta = -\mathbf{e}_r. \tag{2.10}$$

We then denote $s_{rr} \equiv -s$, $s_{\theta\theta} \equiv s$, $s_{r\theta} = s_{\theta r} \equiv \tau$, and using Eqs. (2.5) we obtain

$$\sigma_{rr} = -s - p,$$

$$\sigma_{\theta\theta} = s - p,$$

$$\sigma_{r\theta} = \sigma_{\theta r} = \tau. \tag{2.11}$$

In this notation the equations of motion (2.7) can be rewritten explicitly as

$$\rho\left(\frac{\partial v_r}{\partial t} + v_r\frac{\partial v_r}{\partial r} + \frac{v_\theta}{r}\frac{\partial v_r}{\partial \theta} - \frac{v_\theta^2}{r}\right) = \frac{1}{r}\frac{\partial \tau}{\partial \theta} - \frac{1}{r^2}\frac{\partial}{\partial r}(r^2 s) - \frac{\partial p}{\partial r},$$

$$\rho\left(\frac{\partial v_\theta}{\partial t}+v_r\frac{\partial v_\theta}{\partial r}+\frac{v_\theta}{r}\frac{\partial v_\theta}{\partial \theta}+\frac{v_\theta v_r}{r}\right)=\frac{\partial \tau}{\partial r}+\frac{1}{r}\frac{\partial s}{\partial \theta}-\frac{1}{r}\frac{\partial p}{\partial \theta}+\frac{2\tau}{r}, \tag{2.12}$$

where $\nabla\cdot\boldsymbol{\sigma}$ is calculated explicitly in Appendix A.

Equations (2.4) can be rewritten in components form as

$$D_{ij}^{\mathrm{tot}}=\frac{\partial \epsilon_{ij}^{\mathrm{el}}}{\partial t}+(\mathbf{v}\cdot\nabla\boldsymbol{\epsilon}^{\mathrm{el}})_{ij}+\epsilon_{ir}^{\mathrm{el}}\omega_{rj}+\epsilon_{i\theta}^{\mathrm{el}}\omega_{\theta j}-\omega_{ir}\epsilon_{rj}^{\mathrm{el}}-\omega_{i\theta}\epsilon_{\theta j}^{\mathrm{el}}+D_{ij}^{\mathrm{pl}}. \tag{2.13}$$

Here the components of the total rate of deformation tensor are related to the velocity according to Eqs. (2.1) as

$$D_{rr}^{\mathrm{tot}}\equiv\frac{\partial v_r}{\partial r},\quad D_{\theta\theta}^{\mathrm{tot}}\equiv\frac{\partial_\theta v_\theta+v_r}{r},$$

$$D_{r\theta}^{\mathrm{tot}}\equiv\frac{1}{2}\left[\partial_r v_\theta+\frac{\partial_\theta v_r-v_\theta}{r}\right], \tag{2.14}$$

where the components of the spin tensor $\boldsymbol{\omega}$ in Eq. (2.3) are given by

$$\omega_{rr}=\omega_{\theta\theta}=0,$$

$$\omega_{r\theta}=-\omega_{\theta r}=\frac{1}{2}\left[\frac{\partial_\theta v_r-v_\theta}{r}-\partial_r v_\theta\right]. \tag{2.15}$$

The calculation of the tensor $\mathbf{v}\cdot\nabla\boldsymbol{\epsilon}^{\mathrm{el}}$ is presented in Appendix A; the linear elastic strain components of Eqs. (2.6) are given by

$$\epsilon_{rr}^{\mathrm{el}}=-\frac{p}{2K}-\frac{s}{2\mu},$$

$$\epsilon_{\theta\theta}^{\mathrm{el}}=-\frac{p}{2K}+\frac{s}{2\mu},$$

$$\epsilon_{r\theta}^{\mathrm{el}}=\epsilon_{\theta r}^{\mathrm{el}}=\frac{\tau}{2\mu}. \tag{2.16}$$

Since most of the materials of interest have a large bulk modulus K, i.e., they are almost incompressible, we assume that the density is constant in space and time

$$\rho(\mathbf{r},t)\simeq\rho. \tag{2.17}$$

Therefore, Eq. (2.8) is omitted. Finally, the existence of a free boundary is introduced as the following boundary conditions:

$$\sigma_{ij}n_j=0, \tag{2.18}$$

where $\mathbf{n}$ is the unit normal vector at the free boundary.

B. Viscoplastic constitutive equations: The athermal STZ theory

Up to now we have considered mainly symmetries and conservation laws. A general theoretical framework for the elastoviscoplastic deformation dynamics of amorphous solids should be supplemented with constitutive equations relating the plastic rate of deformation tensor $\mathbf{D}^{\mathrm{pl}}$ to the stress and possibly to other internal state fields. We use the constitutive equations of the recently proposed athermal shear-transformation-zones (STZ) theory [11]. This theory is based on identifying the internal state fields that control plastic deformation. The basic observation is that stressing a disordered solid results in localized reorganizations of groups of particles. These reorganizations occur upon surpassing a local shear threshold, and when they involve a finite irreversible shear in a given direction, we refer to them as an "STZ transition." Once transformed, due to a local redistribution of stresses, the same local region resists further deformation in that direction, but is particularly sensitive to shearing transformation if the local applied stress reverses its direction. Thus an STZ transition is conceived as a deformation unit that can undergo configurational rearrangements in response to driving forces. Furthermore, the stress redistribution that accompanies an STZ transition can induce the creation and annihilation of other local particle arrangements that can undergo further localized transitions; these arrangements are formed or annihilated at a rate proportional to the local energy dissipation (recall that thermal fluctuations are assumed to be absent or negligible). In this sense the interesting localized events need not depend on "preexisting" defects in the material, but can appear and disappear dynamically in a manner that we describe mathematically next.

This picture is cast into a mathematical form in terms of a scalar field Λ that represents the normalized density of regions that can undergo STZ transitions, a tensor $\mathbf{m}$ that represents the difference between the density of regions that can undergo a transition under a given stress and the reversed one, and an effective disorder temperature χ that characterizes the state of configurational disorder of the solid [16]. The present state of the theory relates these internal state fields, along with the deviatoric stress tensor $\mathbf{s}$, to the plastic rate of deformation tensor $\mathbf{D}^{\mathrm{pl}}$ according to

$$\tau_0 D_{ij}^{\mathrm{pl}}=\epsilon_0\Lambda C(\bar{s})\left(\frac{s_{ij}}{\bar{s}}-m_{ij}\right),\quad \bar{s}\equiv\sqrt{\frac{s_{ij}s_{ij}}{2}}. \tag{2.19}$$

In this equation, τ_0 is the elementary time scale of plasticity and ϵ_0 is a dimensionless constant. This equation represents the dependence of the plastic rate of deformation on the current stress s_{ij} and the recent history encoded by the internal state tensorial field $\mathbf{m}$. This field acts as a back stress, effectively reducing the local driving force for STZ transitions, up to the possible state of jamming when the whole parentheses vanish. The parentheses provide information about the orientation of the plastic deformation. The function $\mathcal{C}(\bar{s})$ determines the magnitude of the effect, and is rediscussed below. The field Λ appears multiplicatively since the rate of plastic deformation must be proportional to the density of STZ. The second equation describes the dynamics of the internal back stress field

$$\tau_0\frac{\mathcal{D}m_{ij}}{\mathcal{D}t}=2\frac{\tau_0 D_{ij}^{\mathrm{pl}}}{\epsilon_0\Lambda}-\Gamma(s_{ij},m_{ij})m_{ij}\frac{e^{-1/\chi}}{\Lambda},$$

$$\Gamma(s_{ij},m_{ij}) = \frac{\tau_0 s_{ij} D^{\rm pl}_{ij}}{\epsilon_0 \Lambda}. \tag{2.20}$$

This equation captures the dynamical exchange of stability when the material yields to the applied stress. The equation has a jammed fixed point when the plastic deformation vanishes, in agreement with the state of STZ being all in one orientation, without the production of a sufficient number of new ones in the other orientation. The jammed state is realized when the applied stress is below the yield stress. When the stress exceeds the threshold value the stable fixed point of this equation corresponds to a solution with a nonvanishing plastic rate of deformation. This state corresponds to a situation where enough STZ are being created per unit time to allow a persistent plastic flow. The quantity Γ represents the rate of STZ production in response to the flow $\mathbf{D}^{\rm pl}$. We note that for an isotropic material (before it had been deformed) m_{ij} has the same symmetry of the applied forces s_{ij} as these are responsible for any symmetry breaking. This is the situation considered below. In general, when the **s** changes orientation **m** does not necessarily have the same symmetry.

The next equation, for the density of STZ Λ, is an elementary fixed point equation reading

$$\tau_0 \frac{\mathcal{D}\Lambda}{\mathcal{D}t} = \Gamma(s_{ij},m_{ij})(e^{-1/\chi} - \Lambda). \tag{2.21}$$

The unique fixed point of this equation is the equilibrium solution $\Lambda = e^{-1/\chi}$, where χ is a normalized temperaturelike field which is not necessarily the bath temperature when the system is out of thermal and/or mechanical equilibrium. The last equation is for this variable, reading

$$\tau_0 c_0 \frac{\mathcal{D}\chi}{\mathcal{D}t} = \epsilon_0 \Lambda \Gamma(s_{ij},m_{ij})[\chi_\infty(\tau_0 \bar{D}^{\rm pl}) - \chi],$$

$$\bar{D}^{\rm pl} \equiv \sqrt{\frac{D^{\rm pl}_{ij} D^{\rm pl}_{ij}}{2}}. \tag{2.22}$$

This is a heatlike equation for the configurational degrees of freedom; it is discussed in detail below. Here and elsewhere we assume that quantities of stress dimension are always normalized by the yield stress s_y; this is justified as the STZ equations exhibit an exchange of dynamic stability from jamming to flow at $s=1$, i.e., at a stress that is equal to s_y [11]. The set of Eqs. (2.19)–(2.22) is a tensorial generalization of the effectively scalar equations derived in [11]; such a generalization can be obtained by following the procedure described in Ref. [17]. Here c_0 is a specific heat in units of k_B per particle.

A weak point of the theory is the lack of a first-principle derivation that determines the function $\mathcal{C}(s)$ in Eq. (2.19), which lumps together much of the microscopic physics that controls the stress-dependent rate of STZ transitions. Our theory constrains it to be a symmetric function of s that vanishes with vanishing derivatives at $s=0$, due to the athermal condition that states that no transitions can occur in a direction opposite to the direction of s [11]. This constraint is not sufficient, however, to determine $\mathcal{C}(s)$. To appreciate the uncertainties, recall that STZ transitions are relaxation events, where energy and stress are expected to redistribute. Even without external mechanical forcing, aging in glassy systems involves relaxation events that are poorly understood [18]. The situation is even more uncertain when we deal with dynamics far from mechanical equilibrium. The best one can do at present is to choose the function $\mathcal{C}(s)$ by examining its influence on the resulting macroscopic behaviors [19]. Thus in this paper we will examine the sensitivity of the stability of the expanding cavity to two different choices of $\mathcal{C}(s)$. At present we use the one-parameter family of functions, $\mathcal{C}(\bar{s}) = \mathcal{F}(\bar{s};\zeta)$, proposed in [11]

$$\mathcal{F}(\bar{s};\zeta) \equiv \frac{\zeta^{\zeta+1}}{\zeta!} \int_0^{|\bar{s}|} (|\bar{s}| - s_\alpha) s_\alpha^\zeta \exp(-\zeta s_\alpha) ds_\alpha. \tag{2.23}$$

The integral is over a distribution of transition thresholds whose width is controlled by a parameter ζ (and see [11] for details). For finite values of ζ there can be nonzero subyield plastic deformation for $|s| < 1$. This behavior is well documented in the literature cf. [20] in the context of experimental stress-strain relations and plastic deformations. We note that for s very small or very large,

$$\mathcal{C}(s) \sim s^{\zeta+2} \quad \text{for } s \to 0^+,$$

$$\mathcal{C}(s) \simeq s - 1 \quad \text{for } s \gg 1. \tag{2.24}$$

In Sec. IV C we propose a different one-parameter family of functions $\mathcal{G}(\bar{s};\lambda)$ and study in detail the implications of this different choice on the stability of the expanding cavity.

Equation (2.22) deserves special attention. It is a heatlike equation for the effective disorder temperature χ with a fixed point χ_∞ which is attained under steady state deformation. This reflects the observations of Ref. [21], where the effective temperature χ was shown to attain a unique value in the limit $t_0 \bar{D}^{\rm pl} \to 0$, where t_0 was the particles vibrational time scale. Indeed, in most applications, realistically *imposed* inverse strain rates are much larger than the elementary time scale t_0, i.e., $t_0 \bar{D}^{\rm pl} \ll 1$. If we identify our τ_0 with the vibrational time scale t_0 (see, for example, [22]), we conclude that χ_∞ can be taken as a constant, independent of the plastic rate of deformation. This assumption was adopted in all previous versions of STZ theory. Note also that a low plastic rate of deformation is associated with $s \to 1^+$, i.e., a deviatoric stress that approaches the yield stress from above. However, the situation might be very different in free boundary evolution problems, where high stresses concentrate near the boundary, reaching levels of a few times the yield stress. Estimating χ in the typical range of 0.1–0.15 [22,23], $e^{-1/\chi}$ is in the range 10^{-4}–10^{-3}. Therefore, estimating the other factors in Eq. (2.19), for the high stresses near the free boundary, in the range 1–10, we conclude that $\tau_0 \bar{D}^{\rm pl}$ can reach values in the range 10^{-4}–10^{-2}. Very recent simulations [24] demonstrated convincingly that in this range of normalized plastic rates of deformation, χ_∞ shows a considerable dependence on this rate (see Fig. 1). Since χ affects plastic deformation through an exponential Boltzmann-type factor, even small changes of

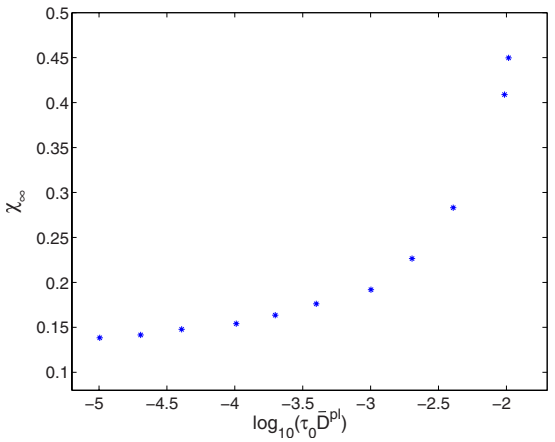

FIG. 1. (Color online) A typical relation between χ_∞ and $\log_{10}(\tau_0 \bar{D}^{\rm pl})$ for a temperature significantly smaller than the glass transition temperature. Data courtesy of T. Haxton and A. Liu. Note that the data were scaled properly.

χ_∞ in Eq. (2.22) can generate significant effects [25]. This issue is of particular importance for the question of stability (and localization) under study since the strain rate sensitivity of χ_∞ might incorporate an instability mechanism; fluctuations in the plastic rate of deformation, caused for example by fluctuations in χ, can induce, through χ_∞, a further localized increase in plastic deformation and so on. This intuitive idea will be studied in the analysis to follow.

The set of Eqs. (2.19)–(2.22) [26] (and slight variants) was shown to capture viscoelastic behavior in a variety of examples. These include small stress and finite plasticity at intermediate stresses [27], a transition to flow at the yield stress (as discussed above) [11], the deformation dynamics of simulated amorphous silicon [22], the necking instability [28], the deformation dynamics near stress concentrations [13], the cavitation instability [14], and strain localization [29]. In this work we focus on the implications of these constitutive equations on the stability of propagating free boundaries in relation to the failure modes of amorphous solids.

C. Unperturbed problem

In this subsection we adapt the general theory to the circular symmetry of the unperturbed expanding cavity problem. We consider an infinite medium with a circular cavity of radius $R^{(0)}(t)$, loaded by a radially symmetric stress σ^∞ at infinity. The superscript (0) in all the quantities denotes the fact that they correspond to the perfectly symmetric case that is going to be perturbed later on. For the perfect circular symmetry the velocity field $\mathbf{v}^{(0)}(\mathbf{r},\theta)$ is purely radial and independent of the azimuthal angle θ, i.e.,

$$v_r^{(0)}(\mathbf{r},t) = v_r^{(0)}(r,t), \quad v_\theta^{(0)}(\mathbf{r},t) = 0. \tag{2.25}$$

This symmetry also implies that

$$\tau^{(0)}(\mathbf{r},t) = 0, \quad D_{r\theta}^{\rm pl(0)}(\mathbf{r},t) = 0, \quad m_{r\theta}^{(0)}(\mathbf{r},t) = 0, \tag{2.26}$$

and all the diagonal components are independent of θ. Equation (2.4), using Eqs. (2.13), (2.14), and (2.16), can be rewritten as

$$\frac{v_r^{(0)}}{r} + \frac{\partial v_r^{(0)}}{\partial r} = -\frac{1}{K}\left(\frac{\partial p^{(0)}}{\partial t} + v_r^{(0)}\frac{\partial p^{(0)}}{\partial r}\right), \tag{2.27}$$

$$\frac{v_r^{(0)}}{r} - \frac{\partial v_r^{(0)}}{\partial r} = \frac{1}{\mu}\left(\frac{\partial s^{(0)}}{\partial t} + v_r^{(0)}\frac{\partial s^{(0)}}{\partial r}\right) + 2D^{\rm pl(0)}, \tag{2.28}$$

where we have defined

$$D_{\theta\theta}^{\rm pl(0)} = -D_{rr}^{\rm pl(0)} \equiv D^{\rm pl(0)}. \tag{2.29}$$

The equations of motion (2.12) reduce to

$$\rho\left(\frac{\partial v_r^{(0)}}{\partial t} + v_r^{(0)}\frac{\partial v_r^{(0)}}{\partial r}\right) = -\frac{1}{r^2}\frac{\partial}{\partial r}(r^2 s^{(0)}) - \frac{\partial p^{(0)}}{\partial r}. \tag{2.30}$$

The boundary conditions are given by

$$\sigma_{rr}^{(0)}(R^{(0)},t) = -p^{(0)}(R^{(0)},t) - s^{(0)}(R^{(0)},t) = 0,$$

$$\sigma_{rr}^{(0)}(\infty,t) = -p^{(0)}(\infty,t) - s^{(0)}(\infty,t) = \sigma^\infty. \tag{2.31}$$

The initial conditions are chosen to agree with the solution of the static linear-elastic problem, i.e.,

$$p^{(0)}(r,t=0) = -\sigma^\infty,$$

$$s^{(0)}(r,t=0) = \sigma^\infty \frac{[R^{(0)}(t=0)]^2}{r^2},$$

$$v_r^{(0)}(r,t=0) = 0. \tag{2.32}$$

This choice reflects the separation of time scales between elastic and plastic responses. This separation of time scales can be written explicitly in terms of the typical elastic wave speed, the radius of the cavity, and the time scale of plasticity as follows:

$$\mathbf{R}^{(0)}(t=0)\sqrt{\frac{\rho}{\mu}} \ll \tau_0 e^{1/\chi}. \tag{2.33}$$

Finally, the rate of the cavity growth is simply determined by

$$\dot{R}^{(0)}(t) = v_r^{(0)}(R^{(0)},t). \tag{2.34}$$

For the circular symmetry, the STZ equations (2.19) and (2.20) reduce to

$$\tau_0 D^{\rm pl(0)} = \epsilon_0 \Lambda^{(0)} \mathcal{C}(s^{(0)})\left(\frac{s^{(0)}}{|s^{(0)}|} - m^{(0)}\right), \tag{2.35}$$

$$\tau_0\left(\frac{\partial m^{(0)}}{\partial t} + v_r^{(0)}\frac{\partial m^{(0)}}{\partial r}\right) = 2\frac{\tau_0 D^{\rm pl(0)}}{\epsilon_0 \Lambda^{(0)}} - \Gamma^{(0)}(s^{(0)},m^{(0)})m^{(0)}\frac{e^{-1/\chi^{(0)}}}{\Lambda^{(0)}}, \tag{2.36}$$

$$\tau_0\left(\frac{\partial \Lambda^{(0)}}{\partial t} + v_r^{(0)}\frac{\partial \Lambda^{(0)}}{\partial r}\right) = \Gamma^{(0)}(s^{(0)},m^{(0)})(e^{-1/\chi^{(0)}} - \Lambda^{(0)}), \tag{2.37}$$

$$\tau_0 c_0 \left(\frac{\partial \chi^{(0)}}{\partial t} + v_r^{(0)} \frac{\partial \chi^{(0)}}{\partial r} \right) = \epsilon_0 \Lambda^{(0)} \Gamma^{(0)}(s^{(0)}, m^{(0)}) [\chi_\infty(\tau_0 D^{\mathrm{pl}(0)}) - \chi^{(0)}]. \quad (2.38)$$

Note that the χ and D^{pl} equations contain a factor of the small STZ density $\epsilon_0 \Lambda^{(0)}$, which implies they are much stiffer than the m and Λ equations. Therefore, whenever the advection terms can be neglected this separation of time scales [13] allows us to replace the equations for $m^{(0)}$ and $\Lambda^{(0)}$ by their stationary solutions

$$m^{(0)} = \begin{cases} \dfrac{s^{(0)}}{|s^{(0)}|} & \text{if } |s^{(0)}| \leqslant 1 \\ \dfrac{1}{s^{(0)}} & \text{if } |s^{(0)}| < 1, \end{cases} \quad (2.39)$$

and

$$\Lambda^{(0)} = e^{-1/\chi^{(0)}}. \quad (2.40)$$

Note that Eq. (2.36) has two stable fixed-point solutions given by Eq. (2.39), where we used Eq. (2.40) and omitted the advection term. The transition between these two solutions corresponds to a transition between a jammed and a plastically flowing state for a deviatoric stress below and above the yield stress, respectively [11]. Equation (2.35) exhibits the corresponding solutions in terms of the plastic rate of deformation, zero and finite, below and above the yield stress, respectively.

The unperturbed problem was studied in detail in Ref. [14]. It was shown that for stresses σ^∞ smaller than a threshold value $\sigma^{\mathrm{th}} \simeq 5$ the cavity exhibits transient dynamics in which its radius approaches a finite value in a finite time. When this happens the material is jammed. On the other hand, for $\sigma^\infty > \sigma^{\mathrm{th}}$ the cavity grows without bound, leading to a catastrophic failure of the material, accompanied by large scale plastic deformations. We stress that this mode of failure by propagating a plastic solution is apparently not related to other recently discovered failure fronts [30]. One major goal of the present study is to analyze the stability of the unbounded growth modes that result from this cavitation. However, we are also interested in the range $\sigma^\infty < \sigma^{\mathrm{th}}$, where the unperturbed theory predicts no catastrophic failure. In this range, a failure can still occur if the cavity, prior to jamming, loses its perfect circular symmetry in favor of relatively slender propagating "fingers." In that case, stress localization near the tips of the propagating fingers can lead to failure via fracture. Such a scenario is typical of brittle fracture where the stress localization due to the geometry of the defect drives crack propagation that might lead to macroscopic failure.

III. LINEAR STABILITY ANALYSIS

We derive here a set of equations for the linear perturbations of the perfect circular symmetry where both inertia and elastic compressibility effects are taken into account. In Appendix B we complement the analysis by considering the quasistatic and incompressible case. This case is mathematically more involved as it contains no explicit time evolution equation for the velocity and the pressure fields. By comparing the results of the two formulations we test for consistency and obtain some degree of confidence in the derivation and the numerical implementation of the equations presented in this section.

A. Equations of motion and kinematics

The quantities involved in the problem are the tensors

$$\mathbf{s} = \begin{pmatrix} -s & \tau \\ \tau & s \end{pmatrix}, \quad \mathbf{D}^{\mathrm{pl}} = \begin{pmatrix} -D^{\mathrm{pl}} & D^{\mathrm{pl}}_{r\theta} \\ D^{\mathrm{pl}}_{r\theta} & D^{\mathrm{pl}} \end{pmatrix}, \quad (3.1)$$

as well as the pressure $p(\mathbf{r},t)$, the velocity $\mathbf{v}(\mathbf{r},t)$ and the location of the free boundary $R(\theta,t)$. We start by expanding all these quantities as follows:

$$\begin{aligned} R(\theta,t) &= R^{(0)}(t) + e^{in\theta} R^{(1)}(t), \\ s(r,\theta,t) &= s^{(0)}(r,t) + e^{in\theta} s^{(1)}(r,t), \\ \tau(r,\theta,t) &= i e^{in\theta} \tau^{(1)}(r,t), \\ p(r,\theta,t) &= p^{(0)}(r,t) + e^{in\theta} p^{(1)}(r,t), \\ v_\theta(r,\theta,t) &= i e^{in\theta} v_\theta^{(1)}(r,t), \\ v_r(r,\theta,t) &= v_r^{(0)}(r,t) + e^{in\theta} v_r^{(1)}(r,t), \\ D^{\mathrm{pl}}(r,\theta,t) &= D^{\mathrm{pl}(0)}(r,t) + e^{in\theta} D^{\mathrm{pl}(1)}(r,t), \\ D^{\mathrm{pl}}_{r\theta}(r,\theta,t) &= i e^{in\theta} D^{\mathrm{pl}(1)}_{r\theta}(r,t). \end{aligned} \quad (3.2)$$

Here all the quantities with the superscript (1) are assumed to be much smaller than their (0) counterparts and n is the discrete azimuthal wave number of the perturbations. The small perturbation hypothesis results in a formal linear decomposition in which each linear mode of wave number n is decoupled from all the other modes. When nonlinear contributions are non-negligible, all the modes become coupled and the formal linear decomposition is invalid.

We expand then the equations of motion (2.12) to first order to obtain

$$\rho \left(\frac{\partial v_r^{(1)}}{\partial t} + v_r^{(0)} \frac{\partial v_r^{(1)}}{\partial r} + v_r^{(1)} \frac{\partial v_r^{(0)}}{\partial r} \right) = -\frac{n\tau^{(1)}}{r} - \frac{1}{r^2} \frac{\partial}{\partial r}(r^2 s^{(1)}) - \frac{\partial p^{(1)}}{\partial r}, \quad (3.3)$$

$$\rho \left(\frac{\partial v_\theta^{(1)}}{\partial t} + v_r^{(0)} \frac{\partial v_\theta^{(1)}}{\partial r} + \frac{v_r^{(0)} v_\theta^{(1)}}{r} \right) = \frac{\partial \tau^{(1)}}{\partial r} + \frac{n s^{(1)}}{r} - \frac{n p^{(1)}}{r} + \frac{2\tau^{(1)}}{r}. \quad (3.4)$$

We proceed by expanding Eqs. (2.4) to first order, which after a simple manipulation yields

$$\frac{\partial v_r^{(1)}}{\partial r} + \frac{-n v_\theta^{(1)} + v_r^{(1)}}{r} = -\frac{1}{K} \left(\frac{\partial p^{(1)}}{\partial t} + v_r^{(0)} \frac{\partial p^{(1)}}{\partial r} + v_r^{(1)} \frac{\partial p^{(0)}}{\partial r} \right), \quad (3.5)$$

$$\frac{-nv_\theta^{(1)}+v_r^{(1)}}{r}-\frac{\partial v_r^{(1)}}{\partial r}=\frac{1}{\mu}\left[\frac{\partial s^{(1)}}{\partial t}+v_r^{(0)}\frac{\partial s^{(1)}}{\partial r}+v_r^{(1)}\frac{\partial s^{(0)}}{\partial r}\right]+2D^{\mathrm{pl}(1)}, \quad (3.6)$$

$$\frac{1}{2}\left[\frac{\partial v_\theta^{(1)}}{\partial r}+\frac{nv_r^{(1)}-v_\theta^{(1)}}{r}\right]=\frac{1}{2\mu}\left[\frac{\partial \tau^{(1)}}{\partial t}+v_r^{(0)}\frac{\partial \tau^{(1)}}{\partial r}-\frac{2s^{(0)}v_\theta^{(1)}}{r}\right]+D_{r\theta}^{\mathrm{pl}(1)}. \quad (3.7)$$

At this point we derive an evolution equation for the dimensionless amplitude of the shape perturbation $R^{(1)}/R^{(0)}$. To that aim we note that

$$\dot{R}=v_r(R)+\mathcal{O}\left[\left(\frac{R^{(1)}}{R^{(0)}}\right)^2\right]. \quad (3.8)$$

Expanding this relation using Eqs. (3.2), we obtain to zeroth order Eq. (2.34) and to first order

$$\dot{R}^{(1)}(t)=v_r^{(1)}(R^{(0)})+R^{(1)}\frac{\partial v_r^{(0)}(R^{(0)})}{\partial r}. \quad (3.9)$$

Therefore, we obtain

$$\frac{d}{dt}\left(\frac{R^{(1)}}{R^{(0)}}\right)=\frac{R^{(1)}}{R^{(0)}}\left[\frac{v_r^{(1)}(R^{(0)})}{R^{(1)}}+\frac{\partial v_r^{(0)}(R^{(0)})}{\partial r}-\frac{v_r^{(0)}(R^{(0)})}{R^{(0)}}\right]. \quad (3.10)$$

This is an important equation since a linear instability manifests itself as a significant increase in $R^{(1)}/R^{(0)}$ such that nonlinear terms become non-negligible. Note that the two last terms in the square brackets are always negative, therefore an instability can occur only if the first term in the square brackets is positive with absolute value larger than the sum of the two negative terms. Moreover, recall that the problem is nonstationary, implying that all the zeroth order quantities depend on time.

In order to derive the boundary conditions for the components of the stress tensor field we expand to linear order the normal unit vector $\mathbf{n}$ (not to be confused with the discrete wave number n) and tangential unit vector $\mathbf{t}$ at the free boundary, obtaining

$$\mathbf{n}=\left(1,-i\frac{R^{(1)}}{R^{(0)}}ne^{in\theta}\right), \quad \mathbf{t}=\left(i\frac{R^{(1)}}{R^{(0)}}ne^{in\theta},1\right). \quad (3.11)$$

Eq. (2.18), expanded to first order, translates to

$$s^{(1)}(R^{(0)})+p^{(1)}(R^{(0)})=-R^{(1)}\left[\frac{\partial s^{(0)}(R^{(0)})}{\partial r}+\frac{\partial p^{(0)}(R^{(0)})}{\partial r}\right], \quad (3.12)$$

$$\tau^1(R^{(0)})=n[s^{(0)}(R^{(0)})-p^{(0)}(R^{(0)})]\frac{R^{(1)}}{R^{(0)}}. \quad (3.13)$$

In addition, all the first order fields decay as $r\to\infty$. The initial conditions are determined by the perturbation scheme that is being studied.

To avoid dealing with an infinite and time-dependent domain we applied the following time-dependent coordinate transformation:

$$\xi=R(t)/r. \quad (3.14)$$

This transformation allows us to integrate the equations in the time-independent finite domain $\xi\in[0,1]$, with the price of introducing new terms in the equations. Controlling the equations at small distances required the introduction of an artificial viscosity on the right-hand side (RHS) of Eq. (2.7). The term introduced is $\rho\eta\nabla^2\mathbf{v}$, with η chosen of the order of the square of space discretization over the time discretization. This introduces zeroth order contributions on the RHS of Eq. (2.30) and first order contributions on the RHS of Eqs. (3.3) and (3.4).

B. Linear perturbation analysis of the STZ equations

The only missing piece in our formulation is the perturbation of the tensorial STZ equations. In addition to the fields considered up to now, the analysis of the STZ equations includes also the internal state fields

$$\mathbf{m}=\begin{pmatrix}-m & m_{r\theta}\\ m_{r\theta} & m\end{pmatrix}, \quad \Lambda \text{ and } \chi. \quad (3.15)$$

Therefore, in addition to Eqs. (3.2) we have

$$m(r,\theta,t)=m^{(0)}(r,t)+e^{in\theta}m^{(1)}(r,t),$$

$$m_{r\theta}(r,\theta,t)=ie^{in\theta}m_{r\theta}^{(1)}(r,t),$$

$$\Lambda(r,\theta,t)=\Lambda^{(0)}(r,t)+e^{in\theta}\Lambda^{(1)}(r,t),$$

$$\chi(r,\theta,t)=\chi^{(0)}(r,t)+e^{in\theta}\chi^{(1)}(r,t). \quad (3.16)$$

We then expand systematically Eqs. (2.19)–(2.23). First, we have

$$\bar{s}=\sqrt{\frac{2(s^{(0)}+e^{in\theta}s^{(1)})^2+2(\tau^{(1)}e^{in\theta})^2}{2}}\simeq|s^{(0)}+e^{in\theta}s^{(1)}|=|s^{(0)}|+e^{in\theta}s^{(1)}\,\mathrm{sgn}(s^{(0)}). \quad (3.17)$$

Accordingly we expand $\mathcal{C}(\bar{s})$ (assuming $s^{(0)}>0$) in the form

$$\mathcal{C}(\bar{s})=\mathcal{C}(s^{(0)}+e^{in\theta}s^{(1)})\simeq\mathcal{C}(s^{(0)})+\frac{d\mathcal{C}}{ds}(s^{(0)})e^{in\theta}s^{(1)}, \quad (3.18)$$

where

$$\frac{d\mathcal{C}}{ds}(s^{(0)})=\frac{\zeta^{\zeta+1}}{\zeta!}\int_0^{|s^{(0)}|}s_\alpha^\zeta\exp(-\zeta s_\alpha)ds_\alpha. \quad (3.19)$$

Substituting the last three equations into Eq. (2.19) and expanding to first order, we obtain

$$\tau_0 D^{\mathrm{pl}(1)} = \epsilon_0 \Lambda^{(0)} \left[\left(\frac{\Lambda^{(1)}}{\Lambda^{(0)}} \mathcal{C}(s^{(0)}) + s^{(1)} \frac{d\mathcal{C}(s^{(0)})}{ds} \right) \times [\mathrm{sgn}(s^{(0)}) - m^{(0)}] - \mathcal{C}(s^{(0)}) m^{(1)} \right], \quad (3.20)$$

$$\tau_0 D_{r\theta}^{\mathrm{pl}(1)} = \epsilon_0 \Lambda^{(0)} \mathcal{C}(s^{(0)}) \left(\frac{\tau^{(1)}}{|s^{(0)}|} - m_{r\theta}^{(1)} \right). \quad (3.21)$$

We then expand Γ in the form

$$\Gamma = \Gamma^{(0)} + e^{in\theta} \Gamma^{(1)} \quad \text{with} \quad \Gamma^{(0)} = \frac{2\tau_0 s^{(0)} D^{\mathrm{pl}(0)}}{\epsilon_0 \Lambda^{(0)}},$$

$$\Gamma^{(1)} = \frac{2\tau_0}{\epsilon_0 \Lambda^{(0)}} \left[s^{(0)} D^{\mathrm{pl}(1)} + s^{(1)} D^{\mathrm{pl}(0)} - \frac{s^{(0)} D^{\mathrm{pl}(0)} \Lambda^{(1)}}{\Lambda^{(0)}} \right]. \quad (3.22)$$

Equation (2.20) is now used to obtain

$$\tau_0 \left(\frac{\partial m^{(1)}}{\partial t} + v_r^{(0)} \frac{\partial m^{(1)}}{\partial r} + v_r^{(1)} \frac{\partial m^{(0)}}{\partial r} \right) = \frac{2\tau_0}{\epsilon_0 \Lambda^{(0)}} \left(D^{\mathrm{pl}(1)} - D^{\mathrm{pl}(0)} \frac{\Lambda^{(1)}}{\Lambda^{(0)}} \right) - \frac{e^{-1/\chi^{(0)}}}{\Lambda^{(0)}} \times \left[\Gamma^{(0)} m^{(1)} + \Gamma^{(1)} m^{(0)} + \Gamma^{(0)} m^{(0)} \left(\frac{\chi^{(1)}}{[\chi^{(0)}]^2} - \frac{\Lambda^{(1)}}{\Lambda^{(0)}} \right) \right], \quad (3.23)$$

and

$$\tau_0 \left(\frac{\partial m_{r\theta}^{(1)}}{\partial t} + v_r^{(0)} \frac{\partial m_{r\theta}^{(1)}}{\partial r} - \frac{m^{(0)} v_\theta^{(1)}}{r} \right) = \frac{2\tau_0 D_{r\theta}^{\mathrm{pl}(1)}}{\epsilon_0 \Lambda^{(0)}} - \Gamma^{(0)} m_{r\theta}^{(1)} \frac{e^{-1/\chi^{(0)}}}{\Lambda^{(0)}}. \quad (3.24)$$

Using Eq. (2.21) we obtain

$$\tau_0 \left(\frac{\partial \Lambda^{(1)}}{\partial t} + v_r^{(0)} \frac{\partial \Lambda^{(1)}}{\partial r} + v_r^{(1)} \frac{\partial \Lambda^{(0)}}{\partial r} \right) = \Gamma^{(0)} \left(e^{-1/\chi^{(0)}} \frac{\chi^{(1)}}{[\chi^{(0)}]^2} - \Lambda^{(1)} \right) + \Gamma^{(1)} (e^{-1/\chi^{(0)}} - \Lambda^{(0)}). \quad (3.25)$$

Expanding $\bar{D}^{\mathrm{pl}}$, similarly to Eq. (3.17), we obtain

$$\bar{D}^{\mathrm{pl}} \simeq |D^{\mathrm{pl}(0)}| + e^{in\theta} D^{\mathrm{pl}(1)} \, \mathrm{sgn}(D^{\mathrm{pl}(0)}). \quad (3.26)$$

Accordingly we expand $\chi_\infty(\tau_0 \bar{D}^{\mathrm{pl}})$ (with $D^{\mathrm{pl}^{(0)}} > 0$) in the form

$$\chi_\infty(\tau_0 \bar{D}^{\mathrm{pl}}) = \chi_\infty(\tau_0 D^{\mathrm{pl}(0)} + e^{in\theta} \tau_0 D^{\mathrm{pl}(1)}) = \chi_\infty(\tau_0 D^{\mathrm{pl}(0)}) + \frac{d\chi_\infty}{d\bar{D}^{\mathrm{pl}}} (\tau_0 D^{\mathrm{pl}(0)}) e^{in\theta} D^{\mathrm{pl}(1)}. \quad (3.27)$$

Then, using Eq. (2.22) we obtain

$$\tau_0 c_0 \left(\frac{\partial \chi^{(1)}}{\partial t} + v_r^{(0)} \frac{\partial \chi^{(1)}}{\partial r} + v_r^{(1)} \frac{\partial \chi^{(0)}}{\partial r} \right) = \epsilon_0 (\Lambda^{(0)} \Gamma^{(1)} + \Gamma^{(0)} \Lambda^{(1)}) [\chi_\infty(\tau_0 D^{\mathrm{pl}(0)}) - \chi^{(0)}] + \epsilon_0 \Lambda^{(0)} \Gamma^{(0)} \times \left[\frac{d\chi_\infty}{d\bar{D}^{\mathrm{pl}}} (\tau_0 D^{\mathrm{pl}(0)}) D^{\mathrm{pl}(1)} - \chi^{(1)} \right]. \quad (3.28)$$

Thus, Eqs. (3.20), (3.21), (3.23)–(3.25), and (3.28) constitute our equations for the dynamics of the first order STZ quantities.

These equations already reveal some interesting features. First note that the coupling between $D^{\mathrm{pl}^{(1)}}$ [which is the quantity that is expected to be of major importance in determining $v_r^{(1)}$ in Eq. (3.10) through Eqs. (3.5)–(3.8)] and $\chi^{(1)}$, $m^{(1)}$ depends on $\mathcal{C}(s^{(0)})$. This means that the strength of the coupling depends on ζ. Similarly, the coupling between $D^{\mathrm{pl}(1)}$ and $s^{(1)}$ depends on $d\mathcal{C}(s^{(0)})/ds$, which is also a function of ζ. These observations demonstrate the importance of the precise form of the function $\mathcal{C}(s)$. This issue is further discussed in Sec. IV C. Finally, note that whenever the advection terms can be neglected, the known separation of time scales [13] allows us to use Eqs. (2.39) and (2.40) and to replace the equations for $m^{(1)}$, $m_{r\theta}^{(1)}$, and $\Lambda^{(1)}$ by their stationary solutions

$$m^{(1)} = \begin{cases} 0 & \text{if } s^{(0)} \leqslant 1 \\ -\dfrac{s^{(1)}}{[s^{(0)}]^2} & \text{if } s^{(0)} > 1, \end{cases} \quad (3.29)$$

$$m_{r\theta}^{(1)} = \begin{cases} \dfrac{\tau^{(1)}}{s^{(0)}} & \text{if } s^{(0)} \leqslant 1 \\ \dfrac{\tau^{(1)}}{[s^{(0)}]^2} & \text{if } s^{(0)} > 1, \end{cases} \quad (3.30)$$

and

$$\Lambda^{(1)} = \frac{\chi^{(1)}}{[\chi^{(0)}]^2} e^{-1/\chi^{(0)}}. \quad (3.31)$$

In the next section we summarize the results of our analysis of the equations derived in Secs. II C, III A, and III B.

IV. RESULTS

We are now ready to present and discuss the results of the stability analysis of the expanding circular cavity. The full set of equations was solved numerically as discussed above. Time and length are measured in units of τ_0 and $R^{(0)}$ $(t=0)$, respectively. Λ and m are set initially to their respective fixed points. The material-specific parameters used are $\epsilon_0=1$, $c_0=1$, $\mu/s_y=50$, $K/s_y=100$, $\rho=1$, $\chi^{(0)}=0.11$, $\chi_\infty=0.13$, and $\zeta=7$, unless otherwise stated. In Sec. IV A we study perturbations of the shape of the cavity and of the effective temperature χ. In Sec. IV B we study the effect of the rate dependence of χ_∞ on the stability analysis and in Sec. IV C we analyze the effect of the stress-dependent rate function $\mathcal{C}(s)$.

A. Perturbing the shape and χ

Studying the linear stability of the expanding cavity can be done by selecting which fields are perturbed and which

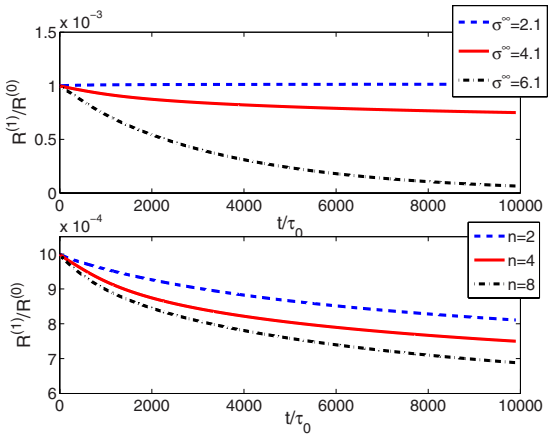

FIG. 2. (Color online) Upper panel: The ratio $R^{(1)}/R^{(0)}$ as a function of time for $n=4$ and $\sigma^{\infty}=2.1$, 4.1, and 6.1. Note that the last value is above the cavitation threshold. Lower panel: The ratio $R^{(1)}/R^{(0)}$ as a function of time for $\sigma^{\infty}=4.1$ and $n=2$, 4, and 8.

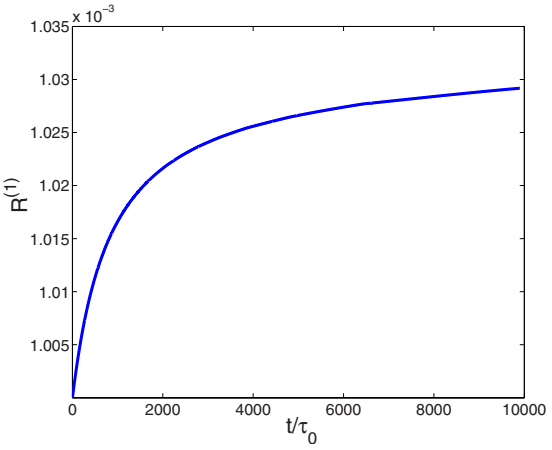

FIG. 3. (Color online) $R^{(1)}$ as a function of time for $\sigma^{\infty}=2.1$ and $n=4$.

are left alone. In practice each of the fields involved in the problem may experience simultaneous fluctuations, including the radius of the cavity itself. Therefore, one of our tasks is to determine which of the possible perturbations leads to a linear instability. To start, we perturb the radius of the expanding cavity at $t=0$ while all the other fields are left alone. In Fig. 2 we show the ratio $R^{(1)}/R^{(0)}$ as a function of time for various loading levels σ^{∞} (both below and above the cavitation threshold) and wave numbers n. The initial amplitude of the perturbation was set to $R^{(1)}/R^{(0)}=10^{-3}$. The observation is that the ratio $R^{(1)}/R^{(0)}$ does not grow in time in all the considered cases where the radius was perturbed, implying that here the circular cavity is stable against shape perturbations. Note that $R^{(1)}/R^{(0)}$ decays faster for larger n and for larger σ^{∞}. Also note that for $\sigma^{\infty}=6.1$, i.e., for unbounded zeroth order expansion, the ratio $R^{(1)}/R^{(0)}$ decays to zero while below the cavitation threshold this ratio approaches a finite value. The latter observations mean that when the material approaches jamming (with $R^{(0)}$ attaining a finite value in a finite time) the perturbation has not yet disappeared entirely.

We stress at this point the nonstationary nature of the problem in which $R^{(0)}(t)$ is an increasing function of time. Thus, even if the absolute magnitude of the amplitude of the shape perturbation $R^{(1)}(t)$ increases with time, an instability is not automatically implied; $R^{(1)}(t)$ should increase sufficiently faster than $R^{(0)}(t)$ in order to imply an instability. To exemplify this feature of the problem, we present in Fig. 3 $R^{(1)}(t)$ for $\sigma^{\infty}=2.1$ and $n=4$. It is observed that even though $R^{(1)}$ increases, the smallness parameter $R^{(1)}/R^{(0)}$ decreases (see Fig. 2). Note also that $R^{(1)}$ does not increase exponentially as expected in stationary linear stability analysis, but rather tends to asymptote to a constant.

Next we have tested the stability of the expanding cavity against initial perturbations in the velocity field or in the stress field. The results were quantitatively similar to those for the shape perturbations summarized in Figs. 2 and 3, all implying linear stability.

In light of these results, we concentrated then on the effect of perturbations in the STZ internal state fields. Since the dynamics of the tensor **m** are mainly determined by the deviatoric stress field s, we focus on fluctuations in the effective disorder temperature χ. This may be the most liable field to cause an instability. Indeed, in Ref. [29] it was shown that χ perturbations control strain localization in a shear banding instability. Qualitatively, an instability in the form of growing fingers involves strain localization as well; plastic deformations are localized near the leading edges of the propagating fingers. In Ref. [29], based on the data of Ref. [23], it was suggested that the typical spatial fluctuations in χ have an amplitude reaching about 30% of the homogeneous background χ. Obviously we cannot treat such large perturbations in a linear analysis and must limit ourselves to smaller perturbations. In Fig. 4 we show the ratio $R^{(1)}/R^{(0)}$ as a function of time for a perturbation of size $\chi^{(1)}/\chi^{(0)}=0.03$, introduced at time $t=0$. The wave number was set to $n=4$ and σ^{∞} was set both below and above the cavitation threshold. First, note that for both loading conditions $R^{(1)}/R^{(0)}$ increases on a short time scale of about $1000\tau_0$, a qualitatively different behavior compared to the system's response to shape perturbations.

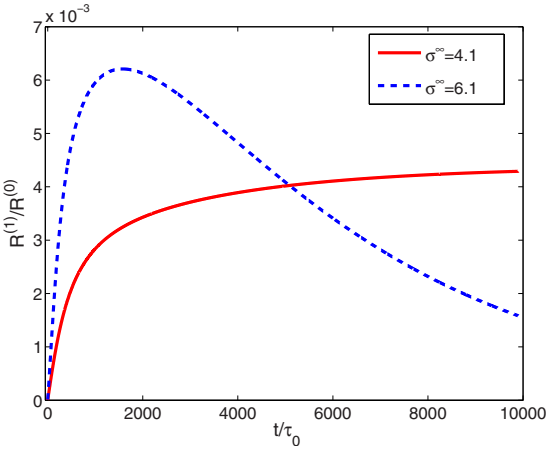

FIG. 4. (Color online) The ratio $R^{(1)}/R^{(0)}$ as a function of time for a perturbation of size $\chi^{(1)}/\chi^{(0)}=0.03$ and $n=4$, introduced at time $t=0$. The solid line corresponds to $\sigma^{\infty}=4.1$ (below the cavitation threshold) and the dashed line corresponds to $\sigma^{\infty}=6.1$ (above the cavitation threshold).

Second, note the qualitatively different response below and above the cavitation threshold. In the former case, $R^{(1)}/R^{(0)}$ increases monotonically, approaching a constant value when $R^{(0)}$ attains a finite value (i.e., jamming). In the latter case, $R^{(1)}/R^{(0)}$ increases more rapidly initially, reaches a maximum, and then decays to 0 in the large t limit. Therefore, in spite of the initial growth of $R^{(1)}/R^{(0)}$, for this magnitude of χ perturbations, the expanding circular cavity is linearly stable; below the cavitation threshold the relative magnitude of the deviation from a perfect circular symmetry $R^{(1)}/R^{(0)}$ tends to a finite constant, i.e., a shape perturbation is "locked in" the material, while above the threshold the cavity retains its perfect circular symmetry in the large t limit. Nevertheless, in light of the significant short time increase in $R^{(1)}/R^{(0)}$ (here up to 0.6%), we increased the initial ($t=0$) χ perturbation to the range $\chi^{(1)}/\chi^{(0)}=0.05-0.06$, in addition to shape perturbations of a typical size of $R^{(1)}/R^{(0)}=0.02-0.03$. In these cases $R^{(1)}/R^{(0)}$ grows above 5%; even more importantly, the field $\chi^{(1)}(\mathbf{r},\theta)$ (as well as other fields in the problem) becomes larger than $0.1\chi^{(0)}(\mathbf{r},\theta)$ near the boundary of the cavity, *invalidating* the small perturbation hypothesis behind the perturbative expansion and signaling a linear instability. Naturally, this breakdown of the linearity condition takes place first near a peak of the ratio $R^{(1)}/R^{(0)}$, similar to the one observed in Fig. 4.

We thus propose that sufficiently large perturbations in the shape of the cavity and the effective disorder temperature χ, but still of formal linear order, may lead to an instability. This dependence on the magnitude of the perturbations in a linear analysis is a result of the nonstationarity of the growth. Another manifestation of the nonstationarity is that even in cases where we detect an instability, it was not of the usual simple exponential type where an eigenvalue changes sign as a function of some parameter (or group of parameters). Combined with the evidence for the existence of large fluctuations in χ [23,29], the present results indicate that it will be worthwhile to study the problem by direct boundary tracking techniques where the magnitude of the perturbation is not limited.

We conclude that the issue of the stability of the expanding cavity can be subtle. Sufficiently small perturbations are stable, though there is a qualitative difference in the response to perturbations in the effective disorder temperature χ, where the ratio $R^{(1)}/R^{(0)}$ increases (at least temporarily), and other perturbations, where $R^{(1)}/R^{(0)}$ decays. We have found that for large enough χ perturbations combined with initial shape perturbations, but still within the formal linear regime, the growth of $R^{(1)}/R^{(0)}$ takes the system beyond the linear regime, making nonlinear effects non-negligible and signaling an instability. This observation is further supported by the existence of large χ fluctuations discussed in [23,29]. Note that none of these conclusions depend significantly on variations in ϵ_0 and c_0. Moreover, perturbing the expanding cavity at times different than $t=0$ or introducing a pressure inside the cavity instead of a tension at infinity did not change any of the results.

B. Effect of the rate dependence of χ_∞

The analysis of Sec. IV A indicates the existence of a linear instability as a result of varying the magnitude of the perturbations, mainly in χ, and not as a result of varying material parameters. Here, and in Sec. IV C, we aim at studying the effect of material-specific properties on the stability of the expanding cavity. Up to now we considered χ_∞ as a constant parameter. However, as discussed in detail in Sec. II B, the plastic rate of deformation near the free boundary can reach values in the range where changes in χ_∞ were observed. Therefore, we repeated the calculations using the function $\chi_\infty(\tau_0\bar{D}^{\mathrm{pl}})$ plotted in Fig. 1. In Fig. 5 we compare $R^{(1)}/R^{(0)}$ as a function of time with and without a plastic rate of deformation dependence of χ_∞, both above and below the cavitation threshold. The initial perturbation has $\chi^{(1)}/\chi^{(0)}=0.03$ and $n=4$. Both below and above the cavitation threshold the plastic rate of deformation-dependent $\chi_\infty(\tau_0\bar{D}^{\mathrm{pl}})$ induces a stronger growth of $R^{(1)}/R^{(0)}$, though the effect is much more significant above the threshold. This is understood as a significantly higher rate of deformation is developed above the cavitation threshold, where unbounded growth takes place [14], compared to below the threshold where the rate of deformation vanishes at a finite time. We note that the dependence of χ_∞ on $\bar{D}^{\mathrm{pl}}$ affects both the zeroth and first order solutions such that $R^{(0)}$ and $R^{(1)}$ increase. Our results show that $R^{(1)}$ is more sensitive to this effect than $R^{(0)}$, resulting in a tendency to lose stability at yet smaller perturbations. We conclude that the tendency of χ_∞ to increase with the rate of deformation plays an important role in the stability of the expanding cavity and might be crucial for other strain localization phenomena as the shear banding instability [29]. Moreover, this material-specific dependence of χ_∞, which was absent in previous formulations of STZ theory, might distinguish between materials that experience catastrophic failure and those that do not, and between materials that fail through a cavitation instability [14] and those who fail via the propagation of fingers that may evolve into cracks. This new aspect of the theory certainly deserves more attention in future work. We note in passing that recently an alternative equation to Eq. (2.22) for the time evolution of

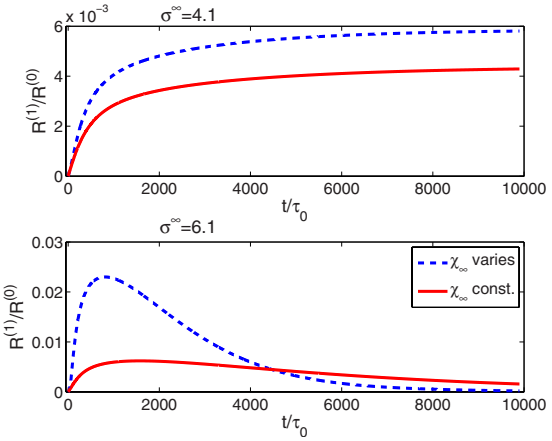

FIG. 5. (Color online) Upper panel: $R^{(1)}/R^{(0)}$ as a function of time for $\sigma^\infty=4.1$ (below the cavitation threshold). The solid line corresponds to a constant χ_∞ and the dashed line corresponds to the plastic rate of deformation dependent $\chi_\infty(\tau_0\bar{D}^{\mathrm{pl}})$ of Fig. 1. The initial perturbation has $\chi^{(1)}/\chi^{(0)}=0.03$ and $n=4$. Lower panel: The same with $\sigma^\infty=6.1$ (above the cavitation threshold).

the effective temperature χ was proposed in light of some available experimental and simulational data [31]. Preliminary analysis of the new equation in relation to the stability analysis performed in this paper indicates that the circular cavity *does* become linearly unstable [32]. A more systematic study of this effect may be a promising line of future investigation.

C. Effect of changing the stress-dependent rate function $\mathcal{C}(s)$

Here we further study the possible effects of details of the constitutive behavior on the macroscopic behavior of the expanding cavity. In this subsection we focus on the material function $\mathcal{C}(s)$. This phenomenological function, as discussed in Sec. II B, describes the stress-dependent STZ transition rates. It is expected to be symmetric and to vanish smoothly at $s=0$ in athermal conditions [11]. The plastic rate of deformation for $s>1$ can be measured in a steady state stress-controlled simple shear experiment. For such a configuration the deviatoric stress tensor is diagonal and the stable fixed points of Eqs. (2.20)–(2.22) imply that the steady state plastic rate of deformation of Eq. (2.19) reads

$$\tau_0 D^{\mathrm{pl}} = \epsilon_0 e^{-1/\chi_\infty} \mathcal{C}(s)\left(1 - \frac{1}{s}\right). \tag{4.1}$$

Therefore, if the steady state relation $\chi_\infty(s)$ is known, $\mathcal{C}(s)$ can be determined from measuring the steady state value of D^{pl} for various $s>1$ (see, for example, [24]). The idea then is to interpolate the $s\to 0^+$ behavior to the $s>1$ behavior with a single parameter that controls the amount of subyield deformation in the intermediate range. In fact, a procedure to measure $\mathcal{C}(s)$ at intermediate stresses was proposed in Ref. [19]. Up to now we used the one-parameter family of functions $\mathcal{F}(s;\zeta)$ of Eq. (2.33), where ζ controls the subyield deformation.

We now aim at studying the effect of choosing another function $\mathcal{C}(s)$. Here we specialize for $\mathcal{C}(\bar{s})=\mathcal{G}(\bar{s};\lambda)$, with

$$\mathcal{G}(\bar{s};\lambda) \equiv \frac{|\bar{s}|^{1+\lambda}}{1+|\bar{s}|^{\lambda}}. \tag{4.2}$$

In Fig. 6 we show $\mathcal{C}(s)$ according to the previous choice of Eq. (2.23) with $\zeta=7$ and also $\mathcal{C}(s)$ according to the present choice of Eq. (4.2) with $\lambda=30$. The different behaviors of $\mathcal{C}(s)$ and $d\mathcal{C}(s)/ds$ near $s=1$ might affect differently $R^{(0)}$ and $R^{(1)}$, thus influencing the stability of the expanding cavity.

In Fig. 7 we compare $R^{(1)}/R^{(0)}$ as a function of time for $\mathcal{C}(s)$ of Eq. (2.23) (previous choice) with $\zeta=7$ and $\mathcal{C}(s)$ of Eq. (4.2) (present choice) with $\lambda=30$, both for a constant χ_∞. An effective temperature perturbation with $\chi^{(1)}/\chi^{(0)}=0.03$ and $n=4$ was introduced at $t=0$ for $\sigma^\infty=4.1$. We observe that $R^{(1)}/R^{(0)}$ grows faster for the present choice compared to the previous one. For the sake of illustration we added the result of a calculation with the plastic rate of deformation-dependent χ_∞ as discussed in Sec. IV B. As expected, the effect is magnified. We conclude that the material-specific function of the stress dependence of the STZ transition rates $\mathcal{C}(s)$ can affect the stability of the expanding cavity, possibly making it unstable for smaller perturbations. Again, the relations between this constitutive property and the macroscopic behavior should be further explored in future work. Bringing into consideration explicit macroscopic measurements, one can constrain the various phenomenological features of the theory of amorphous plasticity. This philosophy provides a complementary approach to obtaining a better microscopic understanding of the physical processes involved.

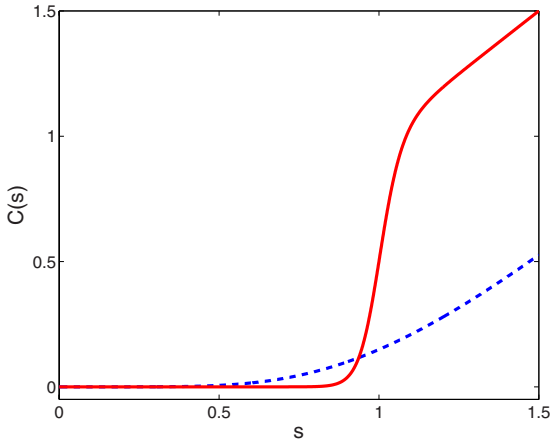

FIG. 6. (Color online) The function $\mathcal{C}(s)$ of Eq. (2.23) with $\zeta=7$ (dashed line) and of Eq. (4.2) with $\lambda=30$ (solid line).

V. CONCLUDING REMARKS

We presented in this paper a detailed analysis of the linear stability of expanding cavity modes in amorphous elastoviscoplastic solids. The stability analysis is somewhat delicate due to the nonstationarity of the problem, thus a perturbation may grow leaving the problem stable if this growth is slower than the growth of the radius of the cavity. The radial sym-

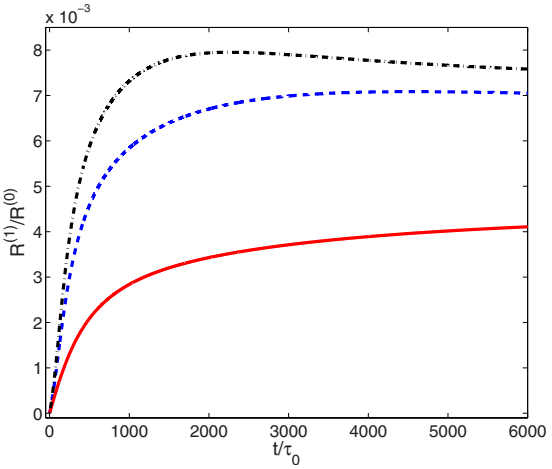

FIG. 7. (Color online) $R^{(1)}/R^{(0)}$ as a function of time for an effective temperature perturbation with $\chi^{(1)}/\chi^{(0)}=0.03$ and $n=4$ for $\sigma^\infty=4.1$. The solid line corresponds to $C(\bar{s})$ of Eq. (2.23) with $\zeta=7$ and the dotted line corresponds to $\mathcal{C}(\bar{s})$ of Eq. (2.23) with $\lambda=30$ (see Fig. 6). In both cases a constant χ_∞ was used. The dotted-dashed line corresponds to $\mathcal{C}(\bar{s})$ of Eq. (4.2) with $\lambda=30$ and the rate-dependent $\chi_\infty(\tau_0\bar{D}^{\mathrm{pl}})$ presented in Fig. 1.

metry of the expanding cavity makes it surprisingly resilient to perturbations in shape, velocity, external strains, and pressure. On the other hand the radial symmetry may be lost due to perturbations in the internal state fields, especially χ, and is also sensitive to details of the constitutive relations that are employed in the STZ theory. In this respect we highlight the role of the plastic rate of deformation-dependent $\chi_\infty(\tau_0\bar{D}^{\mathrm{pl}})$ and of the stress-dependent rates of STZ transitions $\mathcal{C}(s)$. It is difficult to reach conclusive statements, since the growth of perturbations beyond the linear order invalidate the approach taken here, calling for new algorithms involving surface tracking, where the size of perturbations is not limited. Nevertheless the results point out that instabilities are likely, motivating further research into the nonlinear regime. Of particular interest is the possibility to select particular forms of constitutive relations by comparing the predictions of the theory to macroscopic experiments. This appears as a promising approach in advancing the STZ theory towards a final form.

ACKNOWLEDGMENTS

We thank T. Haxton and A. Liu for generously sharing with us their numerical data, and Chris Rycroft for pointing out an error in an early version of the manuscript. This work has been supported in part by the German Israeli Foundation and the Minerva Foundation, Munich, Germany. E.B. acknowledges support from the Center for Complexity Science and the Lady Davis Trust.

APPENDIX A: DIFFERENTIAL OPERATORS IN POLAR COORDINATES

The aim of this appendix is to derive some expressions in polar coordinates that were used earlier in the paper. Specifically, our goal is to calculate the divergence and covariant derivative of a tensor in polar coordinates. We represent a general second order tensor $\mathbf{T}$ in polar coordinates as

$$\mathbf{T} = T_{ij}\mathbf{e}_i \otimes \mathbf{e}_j, \tag{A1}$$

where $\mathbf{e}_i$ and $\mathbf{e}_j$ are unit vectors in polar coordinates and $\otimes$ denotes a tensor product. Using Eqs. (2.9) and (2.10) we obtain

$$\mathbf{e}_r \cdot (\boldsymbol{\nabla} \cdot \mathbf{T}) = \partial_r T_{rr} + \frac{T_{rr}}{r} + \frac{\partial_\theta T_{\theta r}}{r} - \frac{T_{\theta\theta}}{r},$$

$$\mathbf{e}_\theta \cdot (\boldsymbol{\nabla} \cdot \mathbf{T}) = \partial_r T_{r\theta} + \frac{T_{r\theta}}{r} + \frac{T_{\theta r}}{r} + \frac{\partial_\theta T_{\theta\theta}}{r}. \tag{A2}$$

Substituting Eqs. (2.11) for $\mathbf{T}$, we obtain the right-hand sides of Eqs. (2.12).

We proceed now to calculate the covariant derivative of a tensor $\mathbf{v}\cdot\boldsymbol{\nabla}\mathbf{T}$. Using Eqs. (2.9), (2.10), and (A1) we obtain

$$(\mathbf{v} \cdot \boldsymbol{\nabla}\mathbf{T})_{rr} = v_r \partial_r T_{rr} + \frac{v_\theta}{r}\partial_\theta T_{rr} - \frac{v_\theta}{r} T_{r\theta} - \frac{v_\theta}{r} T_{\theta r},$$

$$(\mathbf{v} \cdot \boldsymbol{\nabla}\mathbf{T})_{r\theta} = v_r \partial_r T_{r\theta} + \frac{v_\theta}{r} T_{rr} + \frac{v_\theta}{r}\partial_\theta T_{r\theta} - \frac{v_\theta}{r} T_{\theta\theta},$$

$$(\mathbf{v} \cdot \boldsymbol{\nabla}\mathbf{T})_{\theta r} = v_r \partial_r T_{\theta r} + \frac{v_\theta}{r} T_{rr} + \frac{v_\theta}{r}\partial_\theta T_{\theta r} - \frac{v_\theta}{r} T_{\theta\theta},$$

$$(\mathbf{v} \cdot \boldsymbol{\nabla}\mathbf{T})_{\theta\theta} = v_r \partial_r T_{\theta\theta} + \frac{v_\theta}{r} T_{r\theta} + \frac{v_\theta}{r} T_{\theta r} + \frac{v_\theta}{r}\partial_\theta T_{\theta\theta}. \tag{A3}$$

Substituting Eqs. (2.16) for $\mathbf{T}$ we obtain the needed expressions for $(\mathbf{v}\cdot\boldsymbol{\nabla}\boldsymbol{\epsilon}^{\mathrm{el}})_{ij}$ in Eq. (2.13).

APPENDIX B: THE QUASISTATIC AND INCOMPRESSIBLE CASE

The aim of this appendix is to derive independently the linear perturbation theory for a quasistatic and incompressible case and to compare to the inertial and compressible case in the limit of large bulk modulus K and small velocities v. We show that the results in this limit agree, giving us some degree of confidence in the derivation and the numerical implementation of the equations in both cases.

The unperturbed problem in the quasistatic and incompressible limit was discussed in detail in [13] and is obtained by taking the quasistatic and the incompressible limits in the equations of Sec. II C. Before considering the linear stability problem, we stress that the linear perturbation theory of the STZ equations, presented in Sec. III B, remains unchanged in the present analysis. Only the equations of motion and the kinematic equations are being modified. In the absence of inertial terms, the equations of motion (2.7) become

$$\frac{\partial\tau}{\partial r} + \frac{1}{r}\frac{\partial s}{\partial\theta} - \frac{1}{r}\frac{\partial p}{\partial\theta} + \frac{2\tau}{r} = 0, \tag{B1}$$

$$\frac{1}{r}\frac{\partial\tau}{\partial\theta} - \frac{1}{r^2}\frac{\partial}{\partial r}(r^2 s) = \frac{\partial p}{\partial r}. \tag{B2}$$

To first order we obtain

$$-\frac{1}{r}n\tau^{(1)} - \frac{2s^{(1)}}{r} = \frac{\partial p^{(1)}}{\partial r} + \frac{\partial s^{(1)}}{\partial r}, \tag{B3}$$

$$\frac{\partial\tau^{(1)}}{\partial r} + \frac{n}{r}(s^{(1)} - p^{(1)}) + \frac{2\tau^{(1)}}{r} = 0. \tag{B4}$$

The boundary conditions of Eqs. (3.12) and (3.13) can be further simplified by using the force balance equation to zeroth order and the zeroth order boundary conditions of Eq. (2.31),

$$\frac{\partial p^{(0)}}{\partial r} = -\frac{\partial s^{(0)}}{\partial r} - \frac{2s^{(0)}}{r}. \tag{B5}$$

Substituting into Eqs. (3.12) and (3.13) we obtain

$$s^{(1)}(R^{(0)}) + p^{(1)}(R^{(0)}) = \frac{2s^{(0)}(R^{(0)})R^{(1)}}{R^{(0)}}, \tag{B6}$$

$$\tau^{(1)}(R^{(0)}) = n\frac{2s^{(0)}(R^{(0)})R^{(1)}}{R^{(0)}}. \tag{B7}$$

In addition, all the first order fields decay as $r\to\infty$. In principle, the initial conditions for the partial differential equa-

tions for the first order fields depend on the type of perturbation under consideration. For explicit perturbations in the shape of the cavity, i.e., $R^{(1)}(0) \neq 0$, we can determine the initial stress field by assuming it is simply the quasistatic linear elastic solution corresponding to the perturbed circle. In order to obtain this solution we start with the bi-Laplace equation for the Airy stress function Φ [33],

$$\nabla^2 \nabla^2 \Phi = 0, \tag{B8}$$

where the stress tensor components are given by

$$\sigma_{rr} = \frac{1}{r}\frac{\partial \Phi}{\partial r} + \frac{1}{r^2}\frac{\partial^2 \Phi}{\partial \theta^2},$$

$$\sigma_{\theta\theta} = \frac{\partial^2 \Phi}{\partial r^2}, \quad \sigma_{r\theta} = -\frac{\partial}{\partial r}\left(\frac{1}{r}\frac{\partial \Phi}{\partial \theta}\right). \tag{B9}$$

We then expand the solution in the form

$$\Phi(r,\theta) = \Phi^{(0)}(r) + \Phi^{(1)}(r)e^{in\theta}. \tag{B10}$$

The general solutions for $\Phi^{(1)}(r)$, that also decay at infinity, are given by

$$\Phi^{(1)}(r) = ar^{-n+2} + br^{-n}, \tag{B11}$$

with $n > 0$. Substituting in Eqs. (B9), using the boundary conditions to first order and the following zeroth order solution

$$\sigma^{(0)}_{rr,\theta\theta} = \sigma^{\infty}\left(1 \mp \frac{(R^{(0)})^2}{r^2}\right), \quad \sigma^{(0)}_{r\theta} = 0, \tag{B12}$$

one obtains

$$a = -[R^{(0)}]^n \sigma^{\infty}\frac{R^{(1)}}{R^{(0)}}, \quad b = [R^{(0)}]^{n+2}\sigma^{\infty}\frac{R^{(1)}}{R^{(0)}}. \tag{B13}$$

The resulting stress components are easily calculated, from which we obtain

$$p^{(1)} = 2\sigma^{\infty}\frac{R^{(1)}}{R^{(0)}}(1-n)\left(\frac{R^{(0)}}{r}\right)^n,$$

$$s^{(1)} = \tau^{(1)} = \sigma^{\infty}\frac{R^{(1)}}{R^{(0)}}\left[n(1-n)\left(\frac{R^{(0)}}{r}\right)^n + n(n+1)\left(\frac{R^{(0)}}{r}\right)^{n+2}\right]. \tag{B14}$$

These are the initial conditions for the first order stress tensor components in terms of the initial $R^{(1)}$. To proceed we expand Eqs. (2.4) to first order, assuming $K \to \infty$,

$$\frac{\partial v_r^{(1)}}{\partial r} = -\frac{1}{2\mu}\left[\frac{\partial s^{(1)}}{\partial t} + v_r^{(0)}\frac{\partial s^{(1)}}{\partial r} + v_r^{(1)}\frac{\partial s^{(0)}}{\partial r}\right] - D^{\mathrm{pl}(1)}, \tag{B15}$$

$$\frac{-nv_\theta^{(1)} + v_r^{(1)}}{r} = \frac{1}{2\mu}\left[\frac{\partial s^{(1)}}{\partial t} + v_r^{(0)}\frac{\partial s^{(1)}}{\partial r} + v_r^{(1)}\frac{\partial s^{(0)}}{\partial r}\right] + D^{\mathrm{pl}(1)}, \tag{B16}$$

$$\frac{1}{2}\left[\frac{\partial v_\theta^{(1)}}{\partial r} + \frac{nv_r^{(1)} - v_\theta^{(1)}}{r}\right] = \frac{1}{2\mu}\left[\frac{\partial \tau^{(1)}}{\partial t} + v_r^{(0)}\frac{\partial \tau^{(1)}}{\partial r} - \frac{2s^{(0)}v_\theta^{(1)}}{r}\right] + D_{r\theta}^{\mathrm{pl}(1)}. \tag{B17}$$

In order to propagate $s^{(1)}$ and $\tau^{(1)}$ in time according to these equations we need to know $v_r^{(1)}$ and $v_\theta^{(1)}$ at each time step. However, a basic feature of the quasistatic problem is that there is no evolution equation for the velocity field. Therefore, we must calculate $v_r^{(1)}$ and $v_\theta^{(1)}$ in a different way.

We now discuss the major mathematical difficulty in the quasistatic formulation, i.e., the absence of an explicit evolution equation for the velocity field $\mathbf{v}^{(1)}$. To overcome this difficulty, we should derive new *ordinary differential equations* for $v_r^{(1)}$ and $v_\theta^{(1)}$ such that their time evolution is inherited from the other fields in the problem. The first equation can be obtained readily by adding Eq. (B15) to Eq. (B16),

$$\frac{\partial v_r^{(1)}}{\partial r} + \frac{v_r^{(1)}}{r} - \frac{nv_\theta^{(1)}}{r} = 0, \tag{B18}$$

from which we can extract $v_\theta^{(1)}$,

$$v_\theta^{(1)} = \frac{1}{n}\left(r\frac{\partial v_r^{(1)}}{\partial r} + v_r^{(1)}\right). \tag{B19}$$

In order to obtain the second equation, we eliminate $p^{(1)}$ from the equations by operating with $\frac{\partial}{\partial r}\frac{r}{n}$ on Eq. (B4), adding the result to Eq. (B3), and taking the partial time derivative to obtain

$$2\frac{\partial \dot{s}^{(1)}}{\partial r} + \frac{1}{n}\frac{\partial}{\partial r}\left(r\frac{\partial \dot{\tau}^{(1)}}{\partial r}\right) + \frac{2}{n}\frac{\partial \dot{\tau}^{(1)}}{\partial r} + \frac{n\dot{\tau}^{(1)}}{r} + \frac{2\dot{s}^{(1)}}{r} = 0. \tag{B20}$$

Here and elsewhere the dot denotes partial time derivative. Using Eqs. (B15) and (B17) we obtain

$$\dot{\tau}^{(1)} = 2\mu\left[-D_{r\theta}^{\mathrm{pl}(1)} + \frac{1}{2}\left(\frac{\partial v_\theta^{(1)}}{\partial r} + \frac{nv_r^{(1)} - v_\theta^{(1)}}{r}\right)\right] - v_r^{(0)}\frac{\partial \tau^{(1)}}{\partial r} + \frac{2s^{(0)}v_\theta^{(1)}}{r}, \tag{B21}$$

$$\dot{s}^{(1)} = -2\mu\left(\frac{\partial v_r^{(1)}}{\partial r} + D^{\mathrm{pl}(1)}\right) - v_r^{(1)}\frac{\partial s^{(0)}}{\partial r} - v_r^{(0)}\frac{\partial s^{(1)}}{\partial r}. \tag{B22}$$

Substituting the last two relations in Eq. (B20) and using Eq. (B19), we obtain a *fourth order linear ordinary differential equation* for $v_r^{(1)}$. Since it is straightforward to obtain, but very lengthy, we do not write it explicitly here. It is important to note that the coefficients in this equation depend on time and therefore by solving it at each time step we effectively have a time evolution for the velocity field. Once one solves for $v_r^{(1)}$, Eq. (B19) can be used to calculate $v_\theta^{(1)}$. The fourth order linear differential equation requires four boundary conditions.

The first boundary condition is obtained by using Eq. (B7); with Eqs. (B17), (3.9), and (B19), we obtain a linear relation between $v_r^{(1)}(R^{(0)})$, $\partial_r v_r^{(1)}(R^{(0)})$, and $\partial_r^2 v_r^{(1)}(R^{(0)})$,

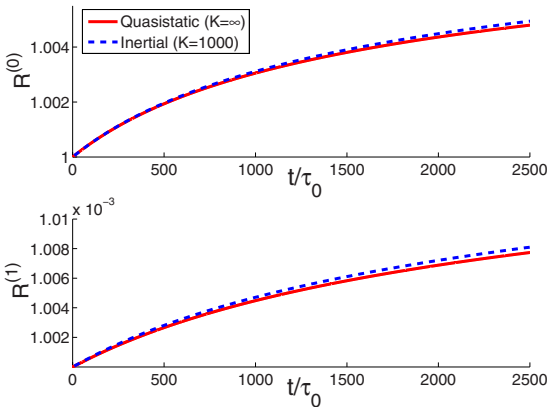

FIG. 8. (Color online) Upper panel: $R^{(0)}$ as a function of time for both the quasistatic (solid line) and the inertial (dashed line) formulations. We used $\sigma^{\infty}=2$, $\zeta=15$, and $K=1000$ in the inertial case to ensure small velocities and almost incompressibility. Lower panel: $R^{(1)}$ as a function of time for both the quasistatic (solid line) and the inertial (dashed line) formulations with a discrete wave number $n=2$. The agreement of the curves in both panels is favorable, where the small differences are attributed to the finite bulk modulus K in the inertial case.

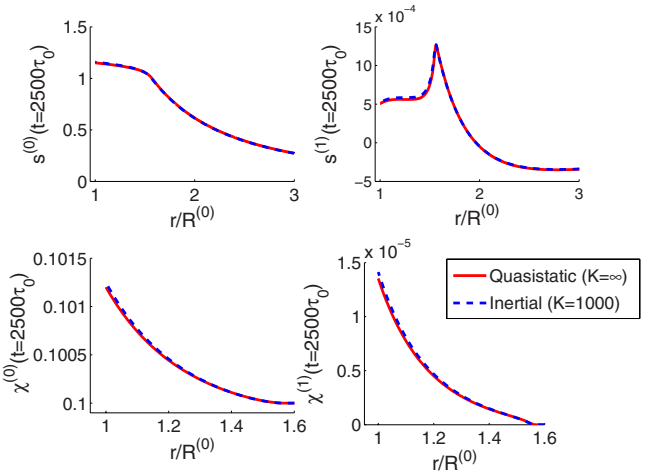

FIG. 9. (Color online) The fields $s^{(0)}(r)$, $s^{(1)}(r)$, $\chi^{(0)}(r)$, and $\chi^{(1)}(r)$ at $t=2500\tau_0$ for both the quasistatic (solid line) and the inertial (dashed line) formulations. The parameters are the same as those of Fig. 8.

which is the required boundary condition. Another boundary condition is obtained by multiplying Eq. (B4) by r, operating with $\frac{\mathcal{D}}{\mathcal{D}t}=\partial_t+v_r^{(0)}\partial_r$ on the result, and using Eq. (B6). Additional simple manipulations result in a linear relation between $v_r^{(1)}(R^{(0)})$, $\partial_r v_r^{(1)}(R^{(0)})$, $\partial_r^2 v_r^{(1)}(R^{(0)})$, and $\partial_r^3 v_r^{(1)}(R^{(0)})$. This is a second boundary relation. Two other boundary conditions are obtained from the requirement that $v_r^{(1)}$ vanishes at ∞ with vanishing derivative

$$v_r^{(1)}(\infty)=0 \quad \text{and} \quad \frac{\partial v_r^{(1)}(\infty)}{\partial r}=0. \tag{B23}$$

With these four boundary conditions the fourth order differential equation can be solved in the following way: at each step we guess $v_r^{(1)}(R^{(0)},t)$ and $\partial_r v_r^{(1)}(R^{(0)},t)$ and use the first two boundary conditions to calculate $\partial_r^2 v_r^{(1)}(R^{(0)},t)$ and $\partial_r^3 v_r^{(1)}(R^{(0)},t)$. Then we use the fourth order differential equation to calculate $v_r^{(1)}$ and $\partial_r v_r^{(1)}$ at ∞. We improve our guess until the solution satisfies Eqs. (B23) (the shooting method).

Thus, we have a complete solution procedure (assuming that the plastic rate of deformation is known, see Sec. III B); for a given $s^{(1)}(r,t)$ and $\tau^{(1)}(r,t)$ we solve the fourth order differential equation for $v_r^{(1)}(r,t)$ following the procedure described above. Having $v_r^{(1)}(r,t)$ we use Eq. (B19) to obtain $v_\theta^{(1)}(r,t)$. Then we use Eqs. (B15), (B17), and (3.9) to propagate $s^{(1)}(r)$, $\tau^{(1)}(r)$, and $R^{(1)}$ in time. We follow the same procedure at each time step to obtain the full time evolution of the perturbation. We note that we have eliminated $p^{(1)}(r,t)$ from the problem, though we can calculate it at every time step using Eq. (B3) or Eq. (B4).

We are now able to compare the quasistatic and incompressible case to the inertial and compressible counterpart in the limit of small velocities and large bulk modulus K. We introduced at $t=0$ a perturbation of magnitude $R^{(1)}/R^{(0)}=10^{-3}$ to the radius of the cavity, with a discrete wave number $n=2$, and solved the dynamics in both formulations. We chose $\sigma^{\infty}<\sigma^{\text{th}}$ such that the velocities are small and $K=1000$ in the inertial case in order to approach the incompressible limit. In Fig. 8 we compare $R^{(0)}$ and $R^{(1)}$ for both the quasistatic and the inertial formulations. The agreement is good. Note that the stability of the expanding cavity depends on the time dependence of the ratio $R^{(1)}/R^{(0)}$; however, we do not discuss the stability yet, but focus on the comparison between the two formulations. In Fig. 9 we further compare the predictions of the two formulations for the zeroth and first order deviatoric stress field s and effective disorder temperature χ at a given time. In all cases the differences are practically indistinguishable. We thus conclude that the quasistatic formulation and the inertial one agree with one another, giving us some confidence in the validity of both. In particular, we conclude that the inertial formulation can be used with confidence also for high velocities where the quasistatic counterpart becomes invalid.

[1] J. Fineberg and M. Marder, Phys. Rep. **313**, 1 (1999).
[2] A. Yuse and M. Sano, Nature (London) **362**, 329 (1993).
[3] M. Adda-Bedia and Y. Pomeau, Phys. Rev. E **52**, 4105 (1995).
[4] E. Bouchbinder, H. G. E. Hentschel, and I. Procaccia, Phys. Rev. E **68**, 036601 (2003).
[5] A. Livne, O. Ben-David, and J. Fineberg, Phys. Rev. Lett. **98**, 124301 (2007).
[6] E. Bouchbinder and I. Procaccia, Phys. Rev. Lett. **98**, 124302 (2007).
[7] L. B. Freund, *Dynamic Fracture Mechanics* (Cambridge Uni-

versity Press, Cambridge, 1998).
[8] A. S. Argon, Acta Metall. **27**, 47 (1979).
[9] A. S. Argon and H. Kuo, Mater. Sci. Eng. **39**, 101 (1979).
[10] M. L. Falk and J. S. Langer, Phys. Rev. E **57**, 7192 (1998).
[11] E. Bouchbinder, J. S. Langer, and I. Procaccia, Phys. Rev. E **75**, 036107 (2007).
[12] E. Bouchbinder, A. Pomyalov, and I. Procaccia, Phys. Rev. Lett. **97**, 134301 (2006).
[13] E. Bouchbinder, J. S. Langer, T. S. Lo, and I. Procaccia, Phys. Rev. E **76**, 026115 (2007).
[14] E. Bouchbinder, T. S. Lo, and I. Procaccia, Phys. Rev. E **77**, 025101 (2008).
[15] S. Santucci, L. Vanel, and S. Ciliberto, Phys. Rev. Lett. **93**, 095505 (2004).
[16] J. S. Langer, Phys. Rev. E **70**, 041502 (2004).
[17] L. Pechenik, Phys. Rev. E **72**, 021507 (2005).
[18] *Jamming and Rheology*, edited by A. J. Liu and S. R. Nagel (Taylor and Francis, New York, 2001).
[19] E. Bouchbinder and T. S. Lo, Phys. Rev. E **78**, 026119 (2008).
[20] J. Lubliner, *Plasticity Theory* (Macmillan, New York, 1990), p. 69–82.
[21] I. K. Ono, C. S. O'Hern, D. J. Durian, S. A. Langer, A. J. Liu, and S. R. Nagel, Phys. Rev. Lett. **89**, 095703 (2002).
[22] E. Bouchbinder, J. S. Langer, and I. Procaccia, Phys. Rev. E **75**, 036108 (2007).
[23] Y. Shi, M. B. Katz, H. Li, and M. L. Falk, Phys. Rev. Lett. **98**, 185505 (2007).
[24] T. K. Haxton and A. J. Liu, Phys. Rev. Lett. **99**, 195701 (2007).
[25] Note that for situations where χ_∞ can become very large one should rewrite Eq. (2.22) such that the term in the square brackets reads $[1-\chi/\chi_\infty]$. This modification is not needed here as we do not consider such situations.
[26] Mainly in situations where all the tensors can be simultaneously diagonalized, resulting in effectively scalar equations.
[27] M. L. Falk and J. S. Langer, MRS Bull. **25**, 40 (2000).
[28] L. O. Eastgate, J. S. Langer, and L. Pechenik, Phys. Rev. Lett. **90**, 045506 (2003).
[29] M. L. Manning, J. S. Langer, and J. M. Carlson, Phys. Rev. E **76**, 056106 (2007).
[30] M. A. Grinfeld, S. E. Schoenfeld, and T. W. Wright, Appl. Phys. Lett. **88**, 104102 (2006).
[31] E. Bouchbinder, Phys. Rev. E **77**, 051505 (2008).
[32] E. Bouchbinder and T. S. Lo (unpublished).
[33] L. D. Landau and E. M. Lifshitz, *Theory of Elasticity*, 3rd ed. (Pergamon, London, 1986).